Electronic Supplementary Material (ESI) for Inorganic Chemistry Frontiers.

Supporting Information

Integration of Metallacycles and Polyoxometalate Macrocycles

Zeng-Kui Zhu,[a] Ya-Yun Lin,[a] Xin-Xiong Li,[a] Dan Zhao,[b,*] and Shou-Tian Zheng[a,*]

[a] State Key Laboratory of Photocatalysis on Energy and Environment, College of Chemistry, Fuzhou University, Fuzhou, Fujian 350108, China.
[b] Fuqing Branch of Fujian Normal University, Fuqing, Fujian, 350300 (China)

*Email: 175721991@qq.com; stzheng@fzu.edu.cn

Contents

Section 1: Synthesis and Methods

Synthesis of 1: A mixture of $K_7Nb_6O_{19}\cdot 13H_2O$ (0.274 g, 0.20 mmol), $Cu(Ac)_2\cdot H_2O$ (0.400 g, 2 mmol), phenylphosphonic acid (0.079 g, 0.5 mmol), 3-Methyl-1,2,4-Triazole (0.083 g, 1 mmol), 3-Ethyl-1,2,4-Triazole (0.039 g, 0.4 mmol), 1.1 ml 2M NaOH and 0.18 ml en was mixed in 8 ml deionized water. After stirred 1 hour, the resulting mixture was sealed in a glass vial (20 ml) and heated at 90 °C for 3 days. After cooling down to room temperature, blue hexagonal lamellar crystals were obtained. The pH values before and after reaction are 10.1 and 9.3 respectively. Yield : ~ 50 mg (~ 18.9%, based on Nb). ICP and elemental analyses (based on dried sample) calcd (found %) for $C_{94}H_{284}Cu_{22}N_{88}Nb_{48}O_{144}$: C, 10.44 (10.13); H, 2.64 (3.51); N, 11.40 (10.93); Cu, 12.93 (12.28); Nb, 41.26 (40.03). IR (KBr, cm^{-1}): 3400m, 3224s, 3127s, 2956m, 2894m, 1645m, 1592s, 1496m, 1461m, 1286m, 1203m, 1107w, 1043s, 987w, 840s, 738s, 619s, 493s, 412s.

Synthesis of 2: A mixture of $K_7Nb_6O_{19}\cdot 13H_2O$ (0.274 g, 0.20 mmol), $Cu(Ac)_2\cdot H_2O$ (0.400 g, 2 mmol), phenylphosphonic acid (0.079 g, 0.5 mmol), 3-Amino-1,2,4-Triazole (0.168 g, 2 mmol), 1.1 ml 2M NaOH and 0.16 ml en was mixed in 8 ml deionized water. After stirred 1 hour, the resulting mixture was sealed in a glass vial (20 ml) and heated at 90 °C for 3 days. After cooling down to room temperature, black block crystals were obtained. The pH values before and after reaction are 9.4 and 9.5, respectively. Yield : ~ 40 mg (~ 18.4%, based on Nb). ICP and elemental analyses (based on dried sample) calcd (found %) for $C_{20}H_{109}N_{32}Na_{13}Cu_8Nb_{48}O_{161}$: C, 2.78 (2.97); H, 1.27 (1.76); N, 5.19 (5.49); Na, 3.46(3.03); Cu, 5.88 (6.21); Nb, 51.61 (49.56). IR (KBr, cm^{-1}): 3401m, 3232s, 3141s, 2954m, 2892m, 1596s, 1540s, 1463w, 1284m, 1218m, 1178w, 1105m, 1043s, 987w, 844s, 734s, 615s, 474s, 412s.

Synthesis of 3: A mixture of $K_7Nb_6O_{19}\cdot 13H_2O$ (0.274 g, 0.20 mmol), $CuCl_2\cdot 2H_2O$ (0.340 g, 2 mmol), Na_2CO_3 (0.105 g, 1 mmol), 1,2,4-Triazole (0.069 g, 1 mmol) and 0.16 ml en was mixed in 8 ml deionized water. After stirred 1 hour, the resulting mixture was sealed in a glass vial (20 ml) and heated at 65 °C for 3days. After cooling down to room temperature, blue purple block crystals were obtained. Yield : ~ 40 mg (~ 16.6%, based on Nb).The pH values before and after reaction are 9.5 and 9.4, respectively. ICP and elemental analyses (based on dried sample) calcd (found %) for $C_{68}H_{264}Cu_{21}K_2N_{76}Na_2Nb_{64}O_{199}$: C,6.41 (6.72); H, 2.09 (3.25); N, 8.36 (8.58); Na, 0.36 (0.41); K, 0.61 (0.54); Cu, 10.48 (10.42); Nb, 46.69 (44.20). IR (KBr, cm^{-1}): 3400m, 3232s, 3139s, 3097s, 2958m, 2894m, 1640m, 1589s, 1521m, 1459w, 1301m, 1180w, 1099m, 1041s, 927w, 850m, 707m, 613s, 518m, 476s, 408s.

Synthesis of 4: A mixture of $K_7HNb_6O_{19}\cdot 13H_2O$ (0.274 g, 0.20 mmol), $Cu(Ac)_2\cdot H_2O$ (0.40 g, 2 mmol), phenylphosphonic acid (0.079 g, 0.5 mmol), 3-Amino-1,2,4-Triazole (0.168 g, 2 mmol), 1.3 ml 2M NaOH and 0.16 ml enMe was mixed in 8 ml deionized water. After stirred 1 hour, the resulting mixture was sealed in a glass vial (20 ml) and heated at 90 °C for 3days. After cooling down to room temperature, black rod crystals were obtained. Yield : ~ 10 mg (~ 3.9%, based on Nb).The pH values before and after reaction are 9.4 and 9.0, respectively. ICP and elemental analyses (based on dried sample) calcd (found %) for $C_{72}H_{257}Cu_{19}KN_{64}Na_4Nb_{48}O_{158}$: C, 8.36 (8.66); H, 2.50 (3.08); N, 8.66 (9.23); Na, 0.89 (0.53); K, 0.38 (0.40); Cu, 11.67 (11.51); Nb, 43.10 (42.28). IR (KBr, cm^{-1}): 3401m, 3228s, 3135s, 2969m, 2884m, 1600s, 1554m, 1519m, 1460w, 1305w, 1246m, 1170w, 1061s, 1026m, 931w, 860s, 708m, 620s, 522s, 481s, 400s.

Crystal data for 1: M_r = 10818.64, triclinic, *P*-1, a = 31.137(2) Å, b = 32.696(2) Å, c = 32.725(2) Å, α = 119.826(2)°, β = 96.085 (3)°, γ = 105.388 (2)°, V = 26715 (3) $Å^3$, Z = 2, ρ = 1.345 g cm^{-3}, GOF = 1.173, ρ(max./min) = 3.354 / -1.946 $eÅ^{-3}$. A total of 391369 reflections were collected, 74964 of which were unique (R_{int} = 0.0461). $R_1(wR_2)$ = 0.0982 (0.2692) for 4054 parameters and 58720 reflections ($I > 2\sigma(I)$). **For 2**: M_r = 8641.26, orthorhombic, *I*mmm, a = 30.150(3) Å, b = 30.349(3) Å, c = 51.839(8) Å, $\alpha = \beta = \gamma = 90°$, V = 47433(10) $Å^3$, Z = 4, ρ = 1.210 g cm^{-3}, GOF =

1.035, ρ(max./min) = 2.158 / - 1.402 eÅ^{-3}. A total of 202336 reflections were collected, 21994 of which were unique (R_{int} = 0.0892). $R_1(wR_2)$ = 0.0953 (0.2414) for 647 parameters and 13425 reflections ($I > 2\sigma(I)$). **For 3**: M_r = 12826.59, monoclinic, $C2/c$, a = 29.987(2) Å, b = 44.601(3) Å, c = 41.073(3) Å, α = 90°, β = 91.247 (10) °, γ = 90°, V = 54920(7) Å^3, Z = 4, ρ = 1.551 g cm^{-3}, GOF = 1.187, ρ(max./min) = 3.671 / - 3.165 eÅ^{-3}. A total of 172040 reflections were collected, 45430 of which were unique (R_{int} = 0.0920). $R_1(wR_2)$ = 0.0993 (0.2647) for 1922 parameters and 30233 reflections ($I > 2\sigma(I)$). **For 4**: M_r = 10346.40, monoclinic, $C2/c$, a = 38.428(5) Å, b = 37.988(5) Å, c = 26.704(3) Å, α = 90°, β = 115.804(15)°, γ = 90°, V = 35095(7) Å^3, Z = 4, ρ = 1.958 g cm^{-3}, GOF = 1.049, ρ(max./min) = 3.182/-2.353 eÅ^{-3}. A total of 115699 reflections were collected, 30969 of which were unique (R_{int} = 0.0599). $R_1(wR_2)$ = 0.0587 (0.1575) for 1629 parameters and 20528 reflections ($I > 2\sigma(I)$). Crystals were collected on a Bruker APEX Due CCD area diffractometer equipped with a fine focus, 2.0 kW sealed tube X-ray source (MoKα radiation, λ = 0.71073 Å) operating at 173(2) K. The empirical absorption correction was based on equivalent reflections. Structures were solved by direct methods followed by successive difference Fourier methods. Computations were performed using SHELXTL and final full-matrix refinements were against F^2. The contribution of disordered solvent molecules to the overall intensity data of structures were treated using the SQUEEZE method in PLATON. CCDC-2045871, 1970659-1970661 contain the supplementary crystallographic data for compounds **1**, **2**, **3** and **4**, respectively.

Water adsorption measurement: As-synthesized samples were exchanged with excessive ethanol 9 times for 3 days. The solvent exchanged sample was then degassed at 80 °C for 12 h under high dynamic vacuum. Water sorption isotherm was recorded at 298K on a micromeritics 3flex Adsorption Analyzer.

Photocatalytic H_2 evolution experiment: The H_2 evolution performance was analysed by a Pyrex reactor connected to the closed gas circulation and evacuation system. It was performed in the Labsolor-6A Reaction System (PrefectLight China) with a 50 mL solution. In a typical experiment, the reactor was filled with 33 mL DMF, 11 mL CH_3CN, 2 mL TEOA and 4 mL H_2O, which containing 0.2 mM [Ir(ppy)2(dtbbpy)][PF_6] and 50 mg compound **1**, **3** or **4**. In this system, the compounds **1**, **3** and **4** were used as the catalysts, the [Ir(ppy)2(dtbbpy)][PF_6] as the photosensitizer, the TEOA as the sacrificial electron donor and the CH_3CN/DMF/H_2O solution was used to solve the solubility issues of photosensitizer [Ir(ppy)$_2$(dtbbpy)][PF_6]. The reaction samples were irradiated by a 300W Xe-light source (λ > 420 nm) and the temperature of the working solution was maintained at 278 K under a flow of circulating water. The amount of evolved hydrogen was measured by Gas Chromatography (GC7900) in every 0.5 h. After reactions, catalysts were separated by centrifugation, washed with CH_3CN several times, and dried at 50 °C in a vacuum oven prior to use for further characterization.

Others: Except that $K_7H[Nb_6O_{19}]\cdot 13H_2O$ precursor was prepared as described in the literature[S1], all chemicals were commercially purchased from *Energy Chemical* and directly used without further purification. PXRD patterns were obtained by using a Ultima IV diffractometer with Cu-*Kα* radiation (λ = 1.5418 Å) in the range 5 - 45°. IR spectra were determined in the range 4000-400 cm^{-1} on a Nicolet IS50 Fourier transform infrared (FT/IR) spectrometer. ICP analyses were conducted on an Ultima2 spectrometer. Elemental analyses for C, H and N were carried out on a Vario MICRO elemental analysis. Luminescence measurements were performed in the solid state at room temperature with Edinburgh Analysis Instruments FLS980.

Section S2 Additional table

Table S1. A summary of known vapour adsorption capacities of polyoxometalate materials.

Compounds[a]	Amount (cm^3g^{-1})	ref
compound **1**	194	This work
compound **3**	230	This work
compound **4**	207	This work
$[Cu(en)_2]_6\{[Cu(en)_2]@\{[Cu_2(trz)_2(en)_2]_6[H_{10}Nb_{68}O_{188}]\}\}$	224	S2
$K_4@\{[Cu_{29}(OH)_7(H_2O)_2(en)_8(trz)_{21}][Nb_{24}O_{67}(OH)_2(H_2O)_3]_4\}$	193	S2
$[Cu(en)_2]@\{[Cu_2(en)_2(trz)_2]_6(Nb_{68}O_{188})\}$	188	S2
$[Zn_{12}(trz)_{20}][SiW_{12}O_{40}]\cdot 11H_2O$	150	S3
$K_3[Cr_3O(OOCH)_6(H_2O)_3][R\text{-}SiW_{12}O_{40}]$	130	S4
$Cu_6(Trz)_{10}(H_2O)_4[H_2SiW_{12}O_{40}]\cdot 8H_2O$	118	S5
$[Cu_4(dpdo)_{12}][H(H_2O)_{27}(CH_3CN)_{12}][PW_{12}O_{40}]_3$	65.1	S6
$K_2[Cr_3O(OOCH)_6(mepy)_3]_2[\alpha\text{-}PMo_{12}O_{40}]\cdot 5H_2O$	56.8	S7
$H_{14}[Na_6(H_2O)_{12}]_4[K_{42}Ge_8W_{72}O_{272}(H_2O)_{60}]\cdot$solvent	52	S8
$[Cu_3(L)_2(H_2O)_4][Cu(dmf)_4(SiW_{12}O_{40})]\cdot 9H_2O$	51.7	S9
$H[Ni(Hbpdc)(H_2O)_2]_2[PW_{12}O_{40}]\cdot 8H_2O\}$	31	S10
$[Co(pn)_3]_4[PNb_{12}O_{40}(VO)_6][OH]_5\cdot 20H_2O$	19.72	S11
$(DODA)_{23}[Mo_{154}O_{462}H_5]\cdot 70H_2O$	16.6	S12
$Cs_{3.6}K_{0.4}[PW_{11}O_{39}(Sn\text{-}OH)]\cdot 8H_2O$	0.31	S13
$K_2[Cr_3O(OOCH)_6(mepy)_3]_2[a\text{-}SiW_{12}O_{40}]\cdot 2H_2O\cdot CH_3OH$	0.03	S14
$Cs_2[Cr_3O(OOCC_2H_5)_6(H_2O)_3]_2$ $[R\text{-}SiW_{12}O_{40}]\cdot 4H_2O$	0.022	S15,S16
$Cs_3H_{0.3}[SiW_{12}O_{40}]_{0.83}\cdot 3H_2O$	0.020	S17

[a] Trz: 1,2,4-triazole; dpdo: 4,4'-bipyridine-N,N'-dioxide; mepy: 4-methylpyridine; L: *N,N*-bis[(2-hydroxy-3-methoxyphenyl) methylidene] hydrazine hydrate ; dmf N,N-Dimethylformamide; H_2bpdc : 2,2'-bipyridyl-3,3'-dicarboxylicacid ; pn: 1,2-diaminopropane ; DODA: dimethyldioctadecylammonium.

References

[S1] M. Filowitz, R. K. C. Ho, W. G. Klemperer, W. Shum, Oxygen-17 nuclear magnetic resonance spectroscopy of polyoxometalates. 1. Sensitivity and resolution**,** *Inorg. Chem.* **1979**, *18*, 93-103.

[S2] Z. K. Zhu, Y. Y. Lin, H. Yu, X. X. Li, S. T. Zheng, Inorganic-organic hybrid polyoxoniobates: polyoxoniobate metal complex cage and cage framework, *Angew. Chem. Int. Ed.* **2019***, 58,* 16864-16868.

[S3] E. L. Zhou, C. Qin, X. L. Wang, K. Z. Shao, Z. M. Su, Steam-assisted synthesis of an extra-stable polyoxometalate-encapsulating metal azolate framework: applications in reagent purification and proton conduction, *Chem. Eur. J.* **2015**, *21*, 13058-13064.

[S4] S. Uchida, R. Kawamoto, N. Mizuno, Recognition of small polar molecules with an ionic crystal of α-Keggin-type polyoxometalate with a macrocation, *Inorg. Chem.* **2006**, *45*, 5136-5144.

[S5] E. L. Zhou, C. Qin, P. Huang, X. L. Wang, W. C. Chen, K. Z. Shao, Z. M. Su, A stable polyoxometalate-pillared metal-organic framework for proton-conducting and colorimetric biosensing, *Chem. Eur. J.* **2015**, *21*, 11894-11898.

[S6] M. Wei, L. Chen, X. Duan, A porous Cu(II)-MOF containing $[PW_{12}O_{40}]^{3-}$ and a large protonated water cluster: synthesis, structure, and proton conductivity, *J. Coord. Chem.* **2014**, *67*, 2809-2819.

[S7] R. Kawahara, S. Uchida, N. Mizuno, Redox-induced reversible uptake-release of cations in porous ionic crystals based on polyoxometalate: cooperative migration of electrons with alkali metal ions, *Chem. Mater.* **2015**, *27*, 2092-2099.

[S8] Z. Li, L. D. Lin, H. Yu, X. X. Li, S. T. Zheng, All-inorganic ionic porous material based on giant spherical polyoxometalates containing core-shell $K_6@K_{36}$-water cage, *Angew. Chem. Int. Ed.* **2018**, *57*, 15777-15781.

[S9] M. L. Wei, J. J. Sun, X. Y. Duan, A complex based on a CuII–schiff-base complex and POM-MOF chain: synthesis, structure and proton conductivity, *Eur. J. Inorg. Chem.* **2014**, 345-351.

[S10] M. Wei, X. Wang, J. Sun, X. Duan, A 3D POM-MOF composite based on Ni(II) ion and 2,2′-bipyridyl-3,3′-dicarboxylic acid: crystal structure and proton conductivity, *J. Solid State Chem.* **2013**, *202,* 200-206.

[S11] J. Hu, Y. Xu, D. Zhang, B. Chen, Z. Lin, C. Hu, A highly symmetric ionic crystal constructed by polyoxoniobates and cobalt complexes for preferential water uptake over alcohols, *Inorg. Chem.* **2017**, *56*, 10844-10847.

[S12] S. Noro, R. Tsunashima, Y. Kamiya, K. Uemura, H. Kita, L. Cronin, T. Akutagawa, T. Nakamura, Adsorption and catalytic properties of the inner nanospace of a gigantic ring-shaped polyoxometalate cluster, *Angew. Chem. Int. Ed.* **2009**, *48*, 8703-8706.

[S13] Y. Miura, H. Imai, T. Yokoi, T. Tastumi, Y. Kamiya, Microporous cesium salts of tetravalent Keggin-type polyoxotungstates $Cs_4[SiW_{12}O_{40}]$, $Cs_4[PW_{11}O_{39}(Sn\text{-}n\text{-}C_4H_9)]$, and $Cs_4[PW_{11}O_{39}(Sn\text{-}OH)]$ and their adsorption properties, *Microporous Mesoporous Mater*. **2013**, *174*, 34-43.

[S14] S. Uchida, R. Eguchi, N. Mizuno, Zeotype organic-inorganic ionic crystals: facile cation exchange and controllable sorption properties, *Angew. Chem. Int. Ed.* **2010**, *49*, 9930-9934.

[S15] A. Lesbani, R. Kawamoto, S. Uchida, N. Mizuno, Control of structures and sorption properties of ionic crystals of $A_2[Cr_3O(OOCC_2H_5)_6(H_2O)_3]_2[\alpha\text{-}SiW_{12}O_{40}]$ (A = Na, K, Rb, NH_4, Cs, TMA), *Inorg. Chem.* **2008**, *47*, 3349-3357.

[S16] C. Jiang, A. Lesbani, R. Kawamoto, S. Uchida, N. Mizuno, Channel-selective independent sorption and collection of hydrophilic and hydrophobic molecules by $Cs_2[Cr_3O(OOCC_2H_5)_6(H_2O)_3]_2[\alpha\text{-}SiW_{12}O_{40}]$ ionic crystal, *J. Am. Chem. Soc.* **2006**, *128*, 14240-14241.

[S17] Y. Ogasawara, S. Uchida, T. Maruichi, R. Ishikawa, N. Shibata, Y. Ikuhara, N. Mizuno, Cubic cesium hydrogen silicododecatungstate with anisotropic morphology and polyoxometalate vacancies exhibiting selective water sorption and cation-exchange properties, *Chem. Mater.* **2013**, *25*, 905-911.

Section S3 Additional Figures

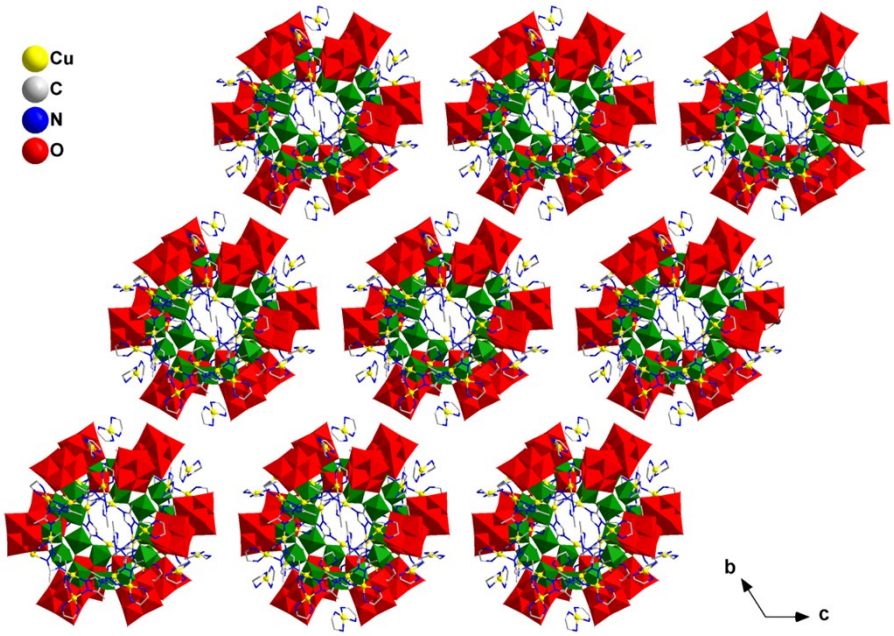

Fig. S1 View of 3D packing structure of **1** along *a*-axis. NbO_6 octahedra: red/green.

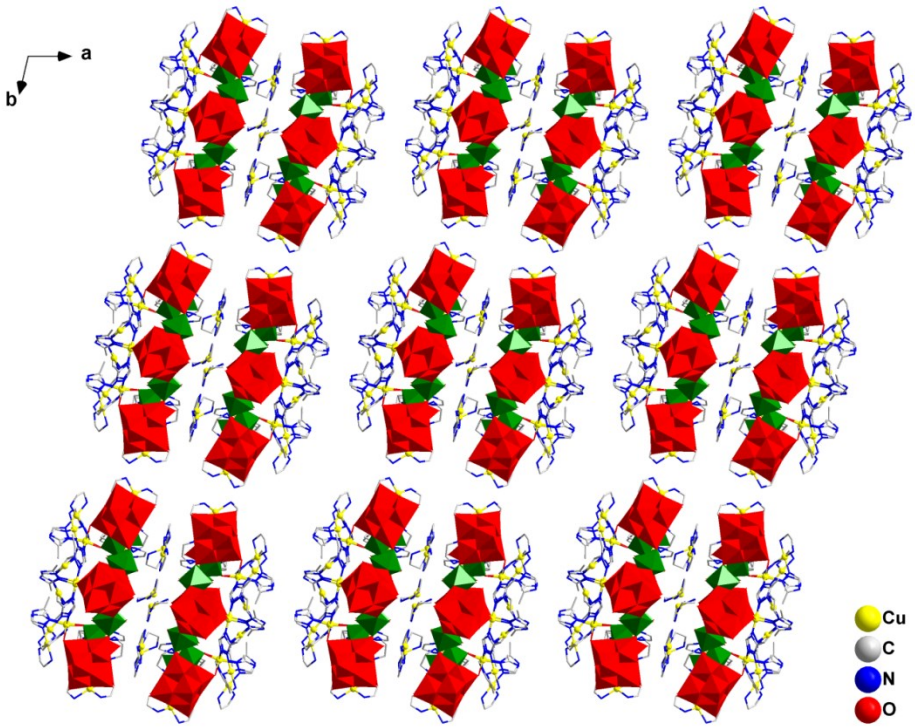

Fig. S2 View of 3D packing structure of **1** along *c*-axis. NbO_6 octahedra: red/green.

In compound **1**, inorganic-organic hybrid PONb macrocycles **1** are arranged in a rhomboic packing mode in the *bc* plane to form an infinite layer (Fig. S1). These layers pack in parallel along a-axis to form whole 3D pack structure with intercluster pores occupied by isolated $[Cu(en)_2]^{2+}$ complexes and neutral guests (Fig. S2), in which the neighboring layers along a-axis are face-to-face or back-to-back to each other.

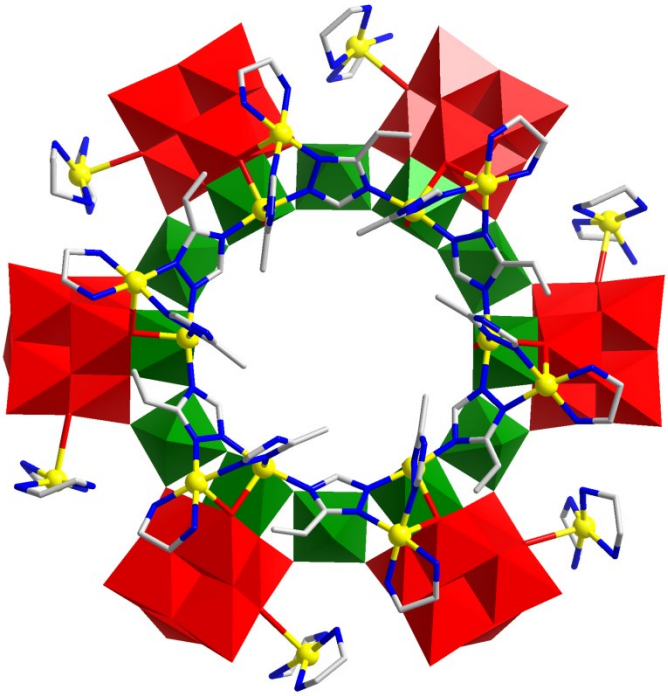

Fig. S3 View of $\{Cu(en)_2\}$-decorating PONb wheel **1**. NbO_6 octahedra: red/green.

In compound **1**, it is interesting to point out that, if Cu-O bond lengths are considered up to 2.75 Å, each Lindqvist hexaniobate $\{Nb_6O_{19}\}$ cluster of PONb wheel **1** can be further decorated by a $[Cu(en)_2]^{2+}$ complex as shown in Fig. S3.

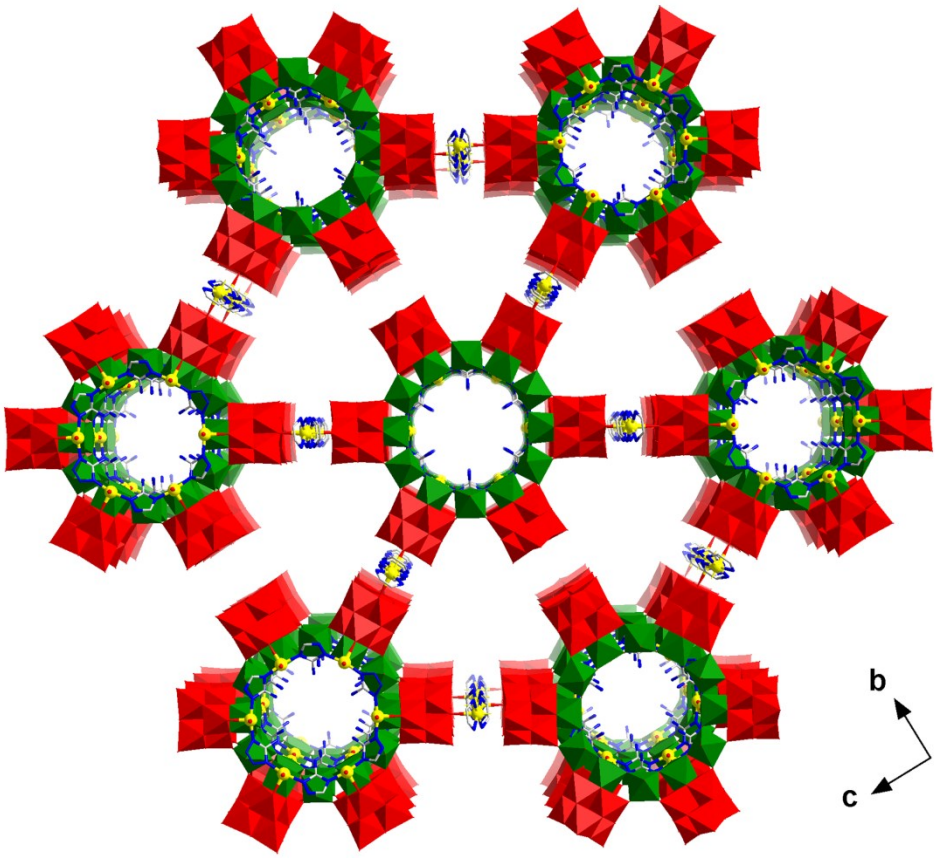

Fig. S4 View of 3D packing structure of **2** along a-axis direction, showing cyclic and trigonal channels. NbO_6 octahedra: red/green.

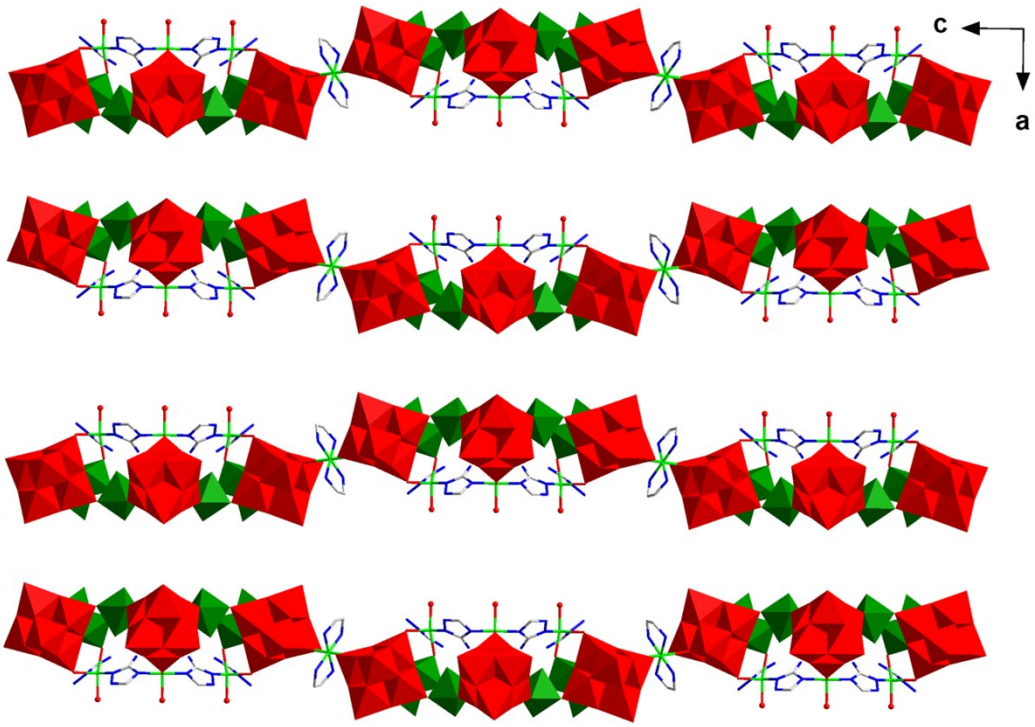

Fig. S5 View of 3D packing structure of **2** along b-axis direction. NbO_6 octahedra: red/green.

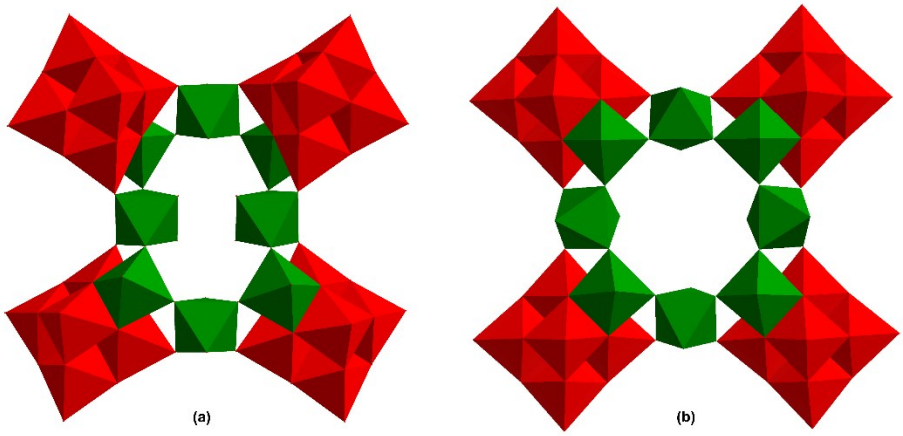

Fig. S6 A structural comparison of 32-nucleairy PONb isomers α-Nb_{32} (a) and β-Nb_{32} (b). NbO_6 octahedra: red/green.

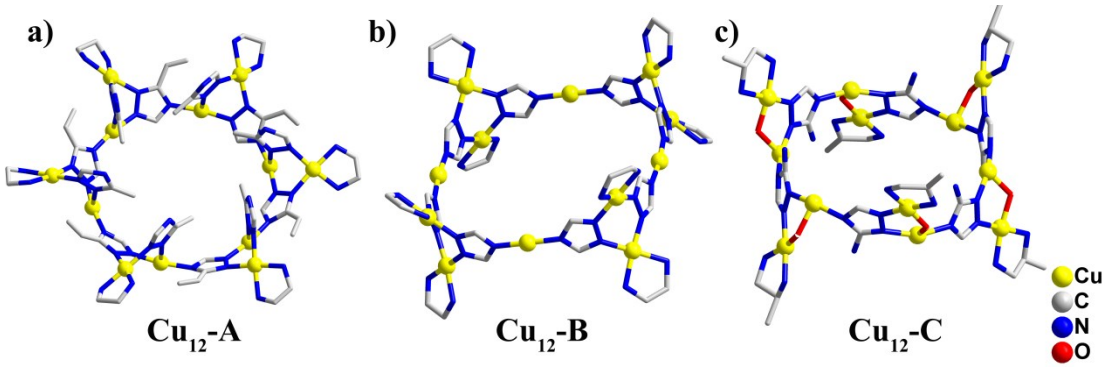

Fig. S7 a)-c) View of metallacycle Cu_{12}-A, Cu_{12}-B and Cu_{12}-C.

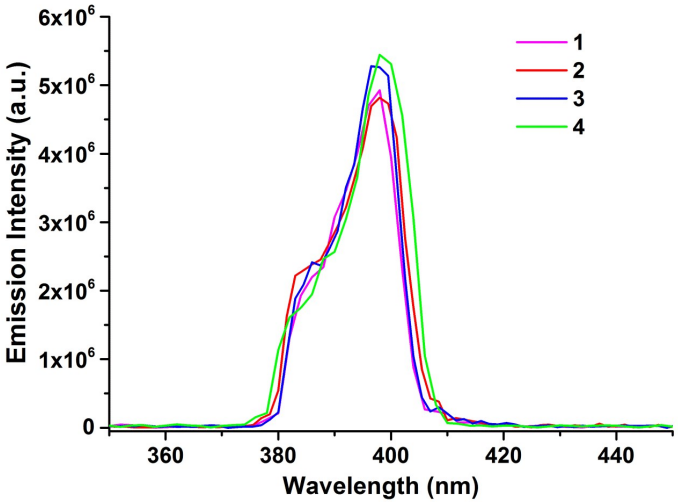

Fig. S8 Emission spectra of compounds-**1**/**2**/**3**/**4** recorded at 300 K (excited at 205 nm).

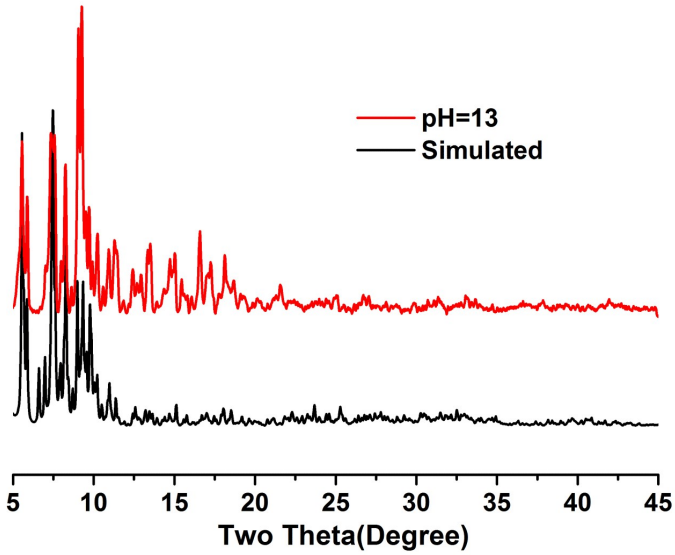

Fig. S9 The stability of compound **3** at pH=13.

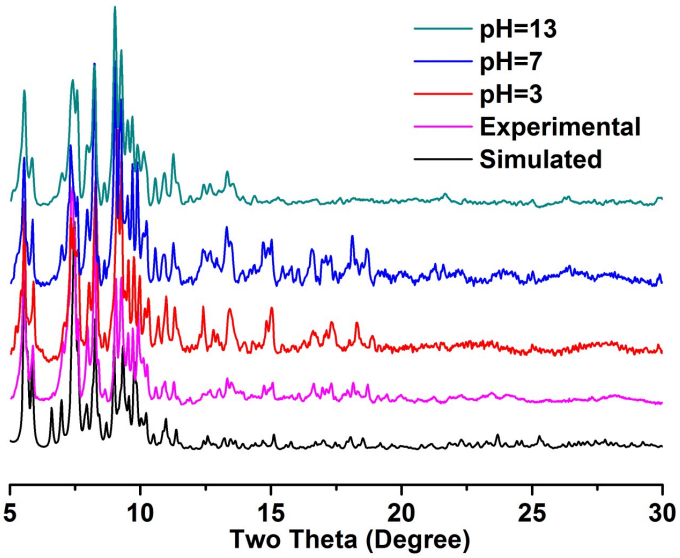

Fig. S10 The pH stabilities in low two theta range in compound **3**.

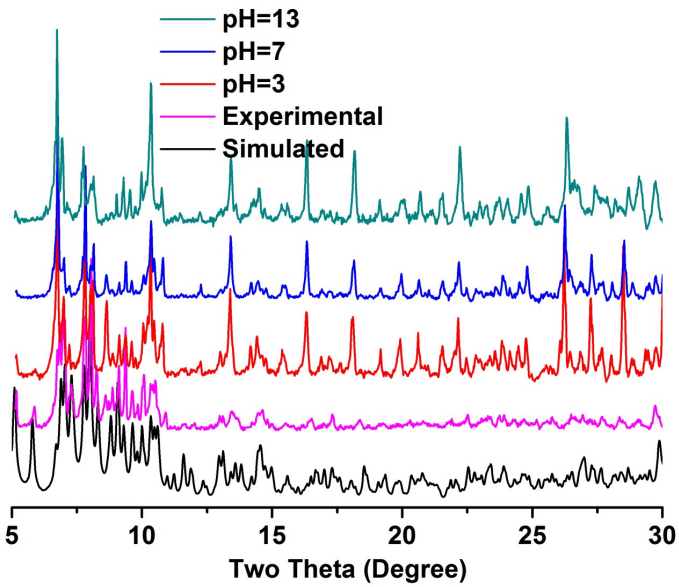

Fig. S11 The pH stabilities in low two theta range in compound **4**.

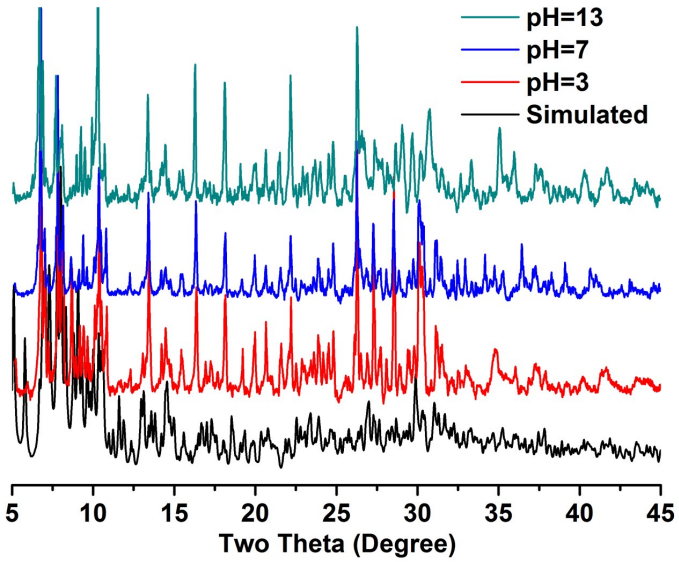

Fig. S12 PXRD of compounds **4** after being soaked in water with different pH values.

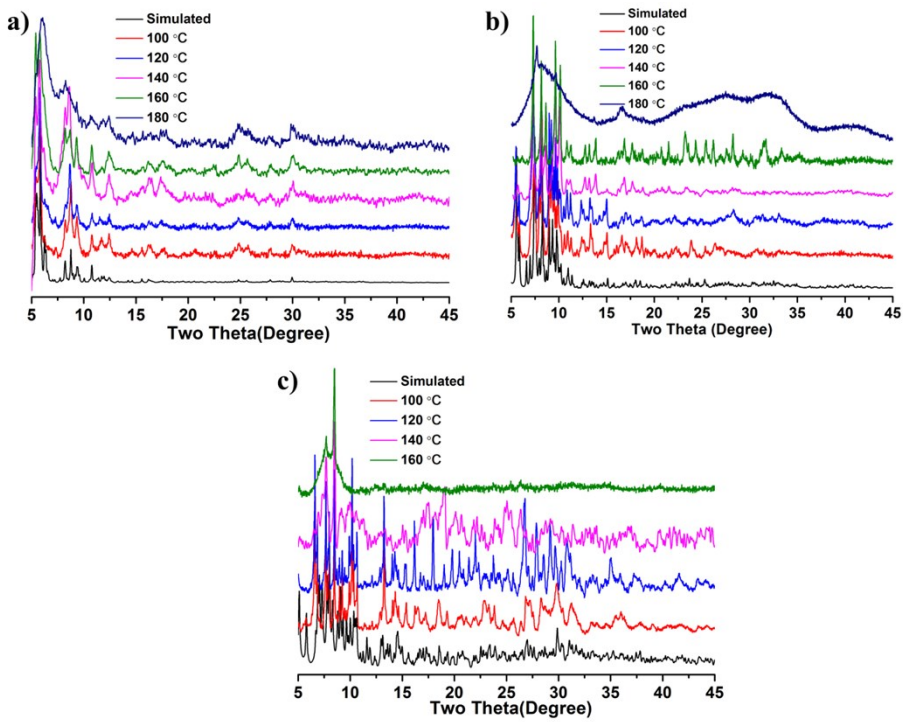

Fig. S13 a)-c) PXRD of compound **1**/**3**/**4** under different temperature, respectively.

As suggestion, we explored the stability of compound **1**/**3**/**4** at different temperatures, and the results show that compound **1**/**3**/**4** can be stabilized to 160, 160 and 120°C, respectively (Fig. S13).

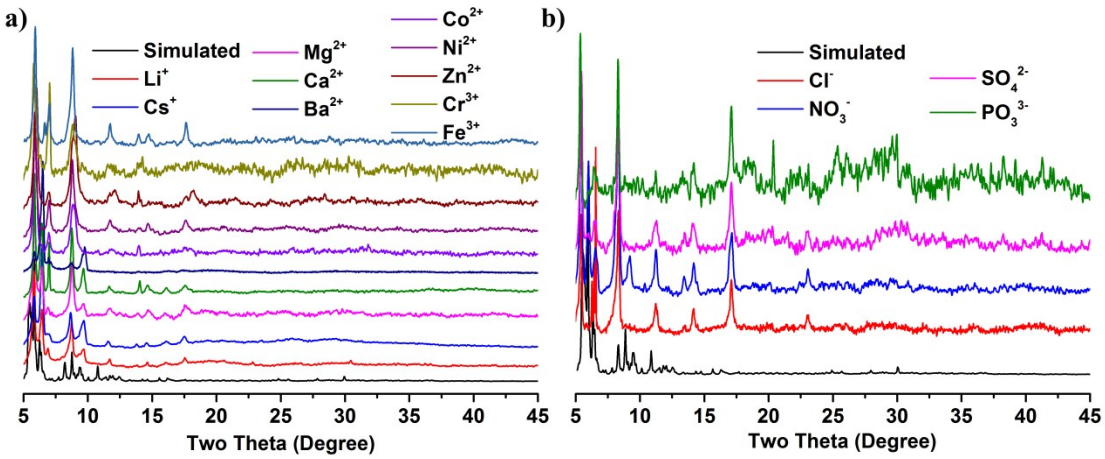

Fig. S14 a) -b) the stability of compound **1** in different cation and anion ions.

We took compound **1** as an example to investigate the stability of this series of compounds in different ions. Since compound **1** exists stably at pH=2, the concentration of H^+ is 0.01M, so we chose 0.01M MClx (x=1, M=Li^+, Cs^+; x=2, M=Mg^{2+}, Ca^{2+}, Ba^{2+}, Co^{2+}, Ni^{2+}, Zn^{2+}; x=3, M=Cr^{3+}, Fe^{3+}) for cationic stability exploration. In the presence of 0.01M monovalent metals (Li^+, Cs^+), divalent metals (Mg^{2+}, Ca^{2+}, Ba^{2+}, Co^{2+}, Ni^{2+}, Zn^{2+}), and trivalent metal ions (Cr^{3+}, Fe^{3+}), compound **1** was immersed in the solutions for 24 hours and then tested for its stability. The results show that compound **1** can exist stably in the presence of cations (Fig. S14a). We also explored the influence of anions. We selected the sodium salt of 0.01M anion (Cl^-, NO_3^-, SO_4^{2-}, PO_3^{3-}) for exploration and found that compound **1** can also stably exist in anions of different valences for 24h (Fig. S14b).

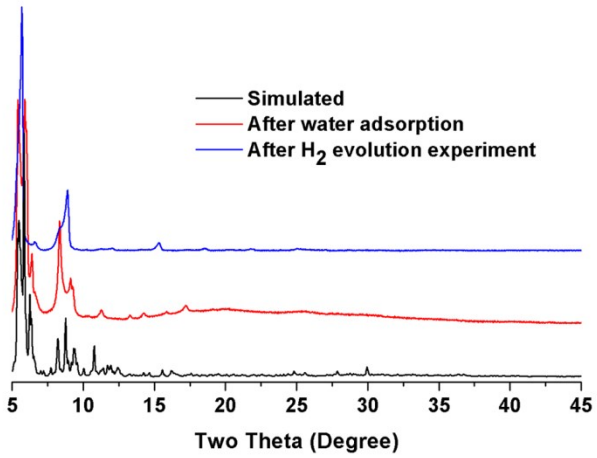

Fig. S15 PXRD patterns of compound **1**.

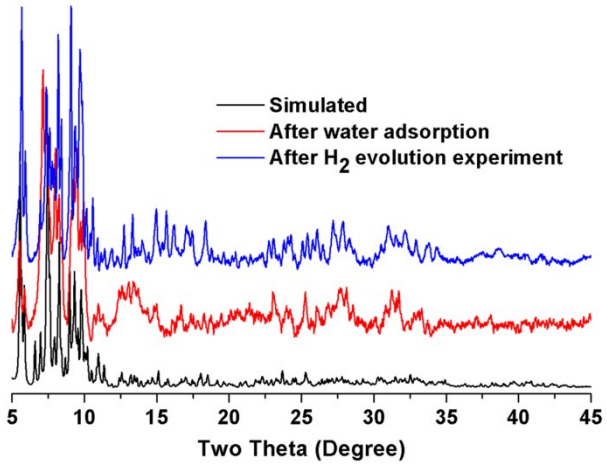

Fig. S16 PXRD patterns of compound **3**.

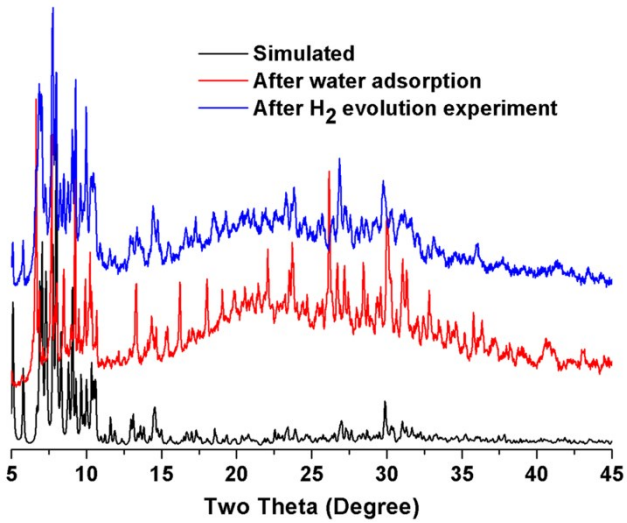

Fig. S17 PXRD patterns of compound **4**.

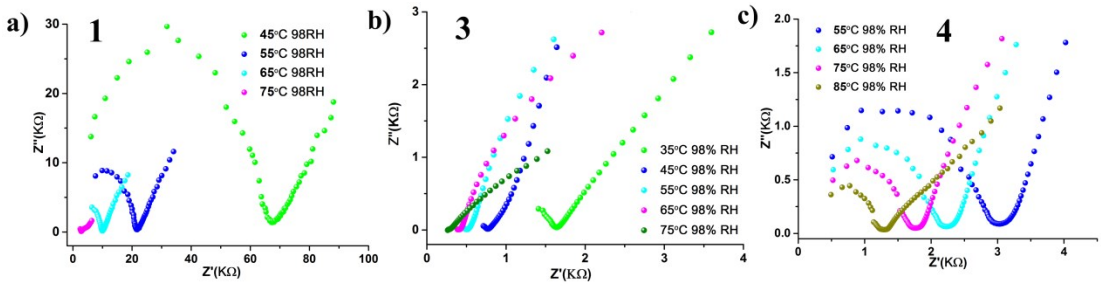

Fig. S18 a)-c) Nyquist plots for compounds **1**/**3**/**4** at different temperatures with 98% RH.

We tested the proton conductivity properties of compounds **1**/**3**/**4**. As shown in the Fig.S18, the proton conductivity of compounds **1**/**3**/**4** at 98% humidity and 75, 75, 85 °C is 3.97×10^{-4}, 1.74×10^{-3} and 5.16×10^{-4} $S\cdot cm^{-1}$, respectively. Since the highest proton conductivity in the field of POMs has reached 10^{-1} $S\cdot cm^{-1}$ (*J. Am. Chem. Soc.* 2020, 142, 13982-13988), the values of these compounds are relatively low.

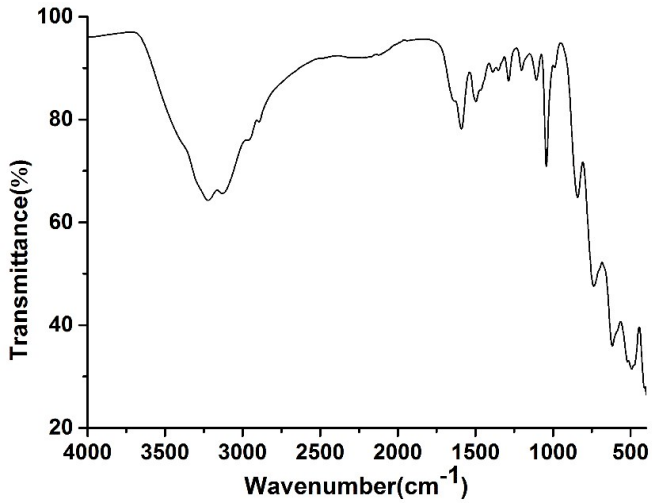

Fig. S19 IR spectrum of compound **1**.

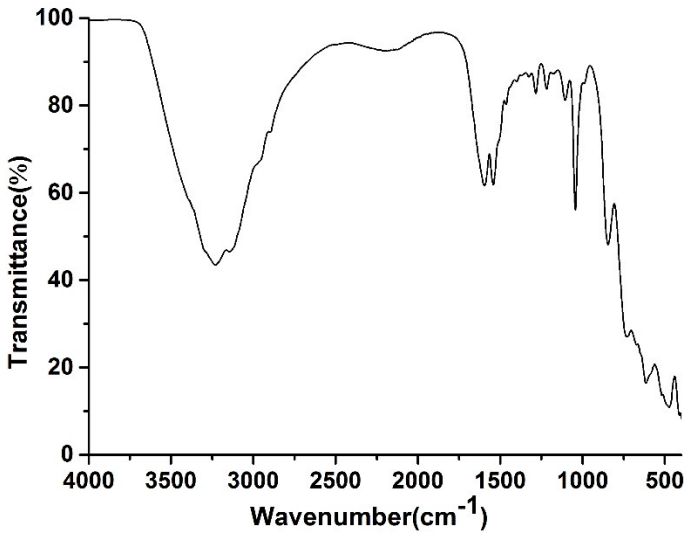

Fig. S20 IR spectrum of compound **2**.

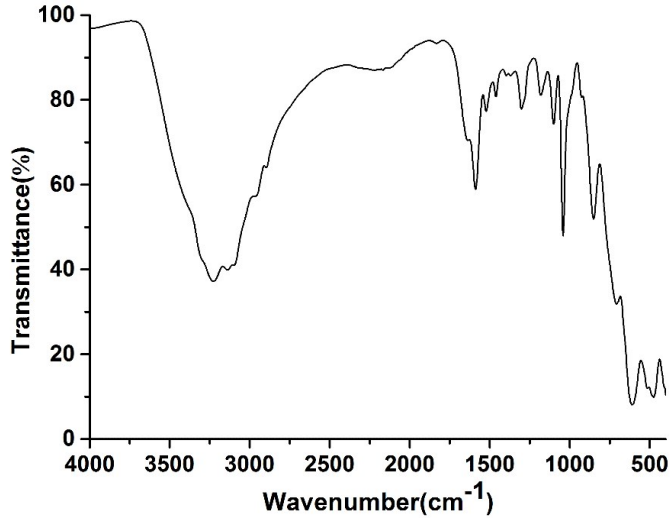

Fig. S21 IR spectrum of compound **3**.

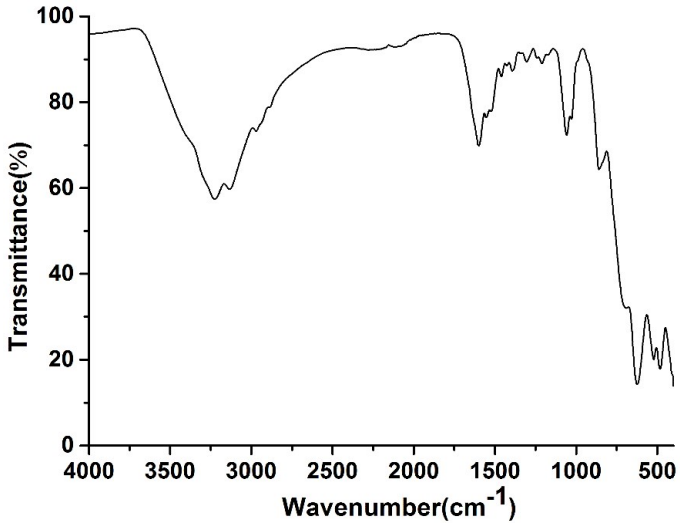

Fig. S22 IR spectrum of compound **4**.

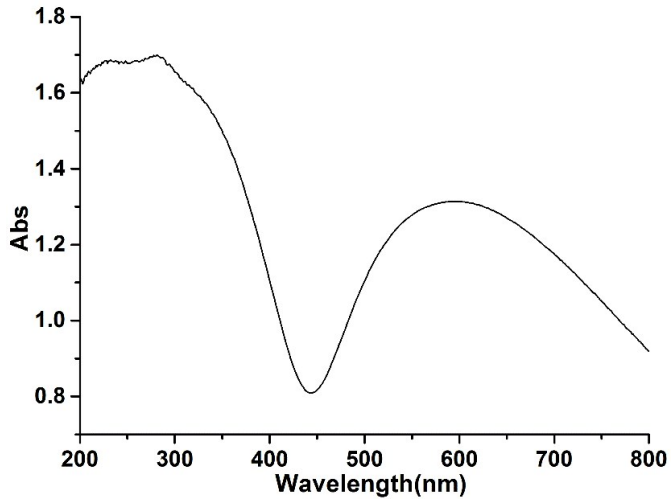

Fig. S23 Solid-state diffuse reflectance UV-vis spectrum of compound **1**.

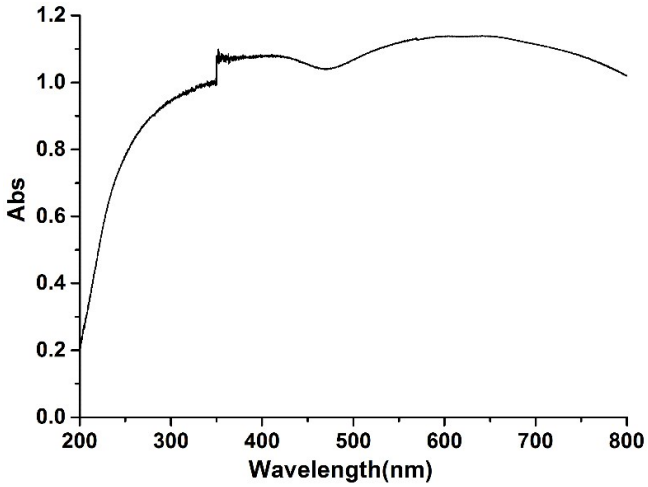

Fig. S24 Solid-state diffuse reflectance UV-vis spectrum of compound **2**.

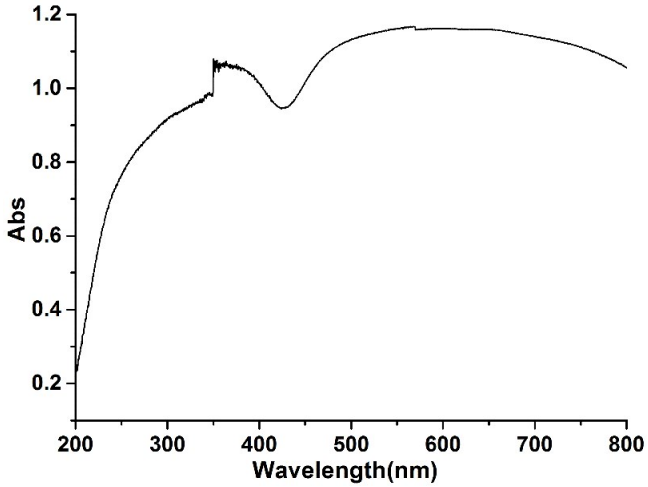

Fig. S25 Solid-state diffuse reflectance UV-vis spectrum of compound **3**.

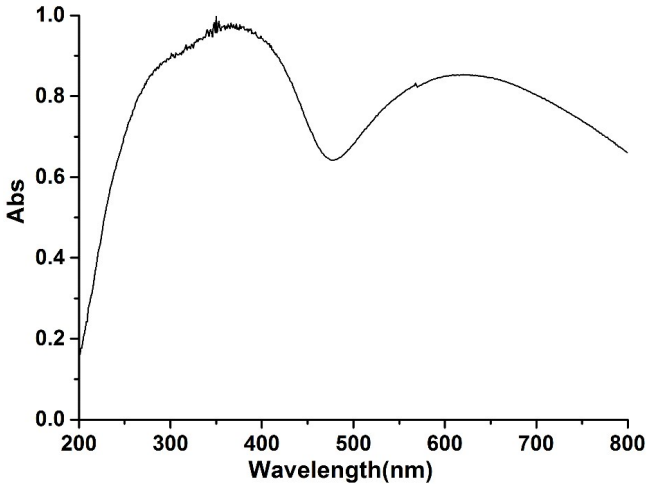

Fig. S26 Solid-state diffuse reflectance UV-vis spectrum of compound **4**.